Flexible Three-Dimensional Anti-Counterfeiting Plasmonic Security Labels: Utilizing Z-Axis-Dependent SERS Readouts to Encode Multi-Layered Molecular Information

Yejing Liu,[1] *Yih Hong Lee,*[1] *Mian Rong Lee,*[1] *Yijie Yang,*[1] *Xing Yi Ling*[1*]

[1] Division of Chemistry and Biological Chemistry, School of Physical and Mathematical Sciences, Nanyang Technological University, 21 Nanyang Link, Singapore 637371.

* To whom correspondence should be addressed. Email: xyling@ntu.edu.sg

Abstract

Current surface-enhanced Raman scattering (SERS)-based anti-counterfeiting strategies primarily encode molecular information in single two-dimensional (2D) planes and under-utilize the three-dimensionality (3D) of plasmonic hot spots. Here, we demonstrate a 3D SERS anti-counterfeiting platform to extend “layered security” capabilities from 2D to 3D. We achieve this capability by combining 3D candlestick microstructures with 3D SERS imaging to fully resolve a at least three layers of encoded information within the same 2D area along the z-axis, notably using only a single probe molecule. Specific pre-designed covert images can only be fully recovered via hyperspectral SERS imaging at pre-determined z values. Furthermore, our 3D SERS anti-counterfeiting security labels can be fabricated on both rigid and flexible substrates, widening their potential usages to curved product surfaces and banknotes.

Keywords: Multi-layer information encoding; three-dimensional surface-enhanced Raman scattering (SERS); plasmonic structures; anti-counterfeiting; security labels

Plasmonic security labels are emerging anti-counterfeiting platforms which can effectively encode multiple identification layers to deter forgery. Information is encoded within micro-/nanostructures by exploiting the unique optical properties arising from the localized surface plasmon resonances (LSPRs) of plasmonic nanostructures.[1-22] By tuning material composition and plasmon coupling between surrounding plasmonic structures, specific structural colors can be generated at the microscale to enable first surface level anti-counterfeiting.[1-8] However, these features alone are insufficient to securely guard products against piracy because the related identifications are visible to public. Enhanced security can be achieved with the use of surface-enhanced Raman scattering (SERS). Intense local electromagnetic fields generated by the LSPRs of the plasmonic structures significantly enhances Raman scattering signals, enabling covert molecular information of reporter molecules adsorbed on plasmonic structures to be read out using SERS imaging techniques. SERS-based anti-counterfeiting has been successfully achieved using polarization-dependent responses as well as using multiple probe molecules with specific and narrow Raman fingerprints.[9-15] Molecular information thus plays a critical role in embedding information in these anti-counterfeiting systems, and is not accessible through the physical features of security labels. Fully decoding them requires knowledge on label design and advanced SERS imaging techniques, leading to a Level 3 Security (L3S) in which information is not attainable unless the security label is decoded using forensic tools with authorization.[23] Currently, the number of identification layers within a platform is increased by adding polarization angles, or increasing the types and concentrations of probe molecules embedded on the plasmonic structures.[9-15] However, these strategies primarily encode molecular information in single two-dimensional (2D) planes and under-utilize the hot spots of SERS substrates in three dimensions (3D).

Extending the “layered security” of SERS anti-counterfeiting platforms from 2D to 3D

further increases the encoded data in the same area. The challenge lies in fabricating a 3D SERS substrate that generates multiple z-axis-dependent SERS readouts which can be fully resolved using SERS imaging techniques. So far, 3D SERS substrates primarily focus on increasing hot spots within the laser confocal volume for enhanced detection sensitivity of probe molecules.[24-31] 3D SERS imaging to resolve molecular information along the z-axis on these substrates is lacking. An earlier work demonstrates using pyramidal micro-structures deposited with Ag nanocubes to generate binary SERS barcodes along z-axis. However, the amount of information stored is limited, and the microstructures are fabricated on rigid glass substrates which break under bending. To enable practical usage of 3D SERS anti-counterfeiting security labels, it is necessary to develop a strategy to build 3D SERS structures on both rigid and flexible substrates.

Here, we introduce a 3D SERS anti-counterfeiting platform with large encoding capacity and high flexibility, achieved by utilizing tailored 3D candlestick-like microstructures and high-resolution 3D SERS imaging to fully resolve readouts along z-axis. Our aim is to maximize the encoding capacity of SERS-based platforms using a single type of probe molecule by extending the "layered security" of plasmonic security labels from 2D to 3D. Plasmonic candlestick microstructures comprising a nanopillar on top of a dish and a pedestal are used as building blocks for 3D anti-counterfeiting security labels. During the thermal evaporation of Ag, the dish in the middle shields Ag deposition on the bottom pedestal and thus generates a microstructure with non-uniform Ag coating in the z-direction. Such anisotropic Ag deposition on the candlestick microstructures creates a z-dependent SERS readout. By using microstructures with different heights, we stack multiple layers of covert SERS images at different focal planes along z-axis (z-dependent SERS). We demonstrate at least three layers of information encoding for our 3D SERS security labels using just one type of probe molecules. We further fabricate our 3D SERS security labels on

flexible polyethylene terephthalate (PET) films without reducing the encoding capability and decoding accuracy, making this anti-counterfeiting platform attractive for practical applications.

Results and Discussion

Fabrication Methods & Z-dependent SERS Readouts

We use two-photon laser lithography to fabricate high aspect ratio polymer-based 3D microstructures resembling candlesticks (Figure 1A). These candlestick microstructures comprise three components, including a 1-μm tall nanopillar at the top, a 2-μm tall middle dish, and a 2-μm tall base pedestal (Figure 1B-ii and Figure S1). The widths of the nanopillar tip and the middle dish are 500 nm and 2.3 μm respectively (Figure 1B-ii). The fabricated candlestick microstructures are then coated with 100-nm Ag via thermal evaporation, and rendered SERS-active by functionalizing the Ag-coated microstructures with a monolayer of 4-methylbenzenethiol (4-MBT) probe molecules. Thermal evaporation of Ag generates nanoscale asperities serving as hot spots for SERS imaging on the 3D microstructures (Figure S2). The candlestick architecture allows us to achieve 3D SERS activity for anti-counterfeiting: Ag deposition on such microstructures are selectively coated on the nanopillar and upper half of the dish, evident from the stronger SEM contrast from these regions of the microstructures (Figure 1B-i).

Next, we characterize the plasmonic properties of the candlestick microstructure using cathodoluminescence spectroscopy. A fast electron beam excites the microstructures to trigger photon emission generated via the radiative decay of localized surface plasmon resonances (LSPRs), allowing the radiative plasmon modes of the Ag-coated candlestick microstructures to be identified at the single structure level. Strong emission is observed at ~530 nm from the microstructure's cathodoluminescence wavelength-filtered photon map, and the corresponding spectrum shows an

intense emission peak centered at ~537 nm as well as a weaker shoulder peak centered at ~658 nm (Figure 2A). The appearance of two broad peaks likely arises from coupling of Ag nanoparticles' plasmon modes.[32-35] There is no emission observed from the flat areas of the substrates, indicating that the observed emission arises from the microstructure. Based on the strong emission at ~537 nm, we select 532-nm as the laser excitation source to measure the SERS response from our 3D candlestick microstructures.

To evaluate the suitability of the candlestick microstructures for 3D anti-counterfeiting, we analyze the SERS readouts of various x-y focal planes along different z positions. Z positions are labeled such that larger z values correspond to longer distance between the focal plane and the base of the substrate. The SERS spectrum of a candlestick microstructure exhibit two typical 4-MBT vibrational modes at 1078 cm^{-1} and 1584 cm^{-1} (Figure 2B). The 1078 cm^{-1} band is attributed to a combination of phenyl ring-breathing, C-H in-plane bending, and C-S stretching, whereas the 1584 cm^{-1} band arises from phenyl stretching motion. To monitor SERS readouts on different focal planes, we select the 1078 cm^{-1} band to generate SERS x-y images at various z positions. We first combine 36 x-y SERS images scanned at 0.25-μm z-intervals to reconstruct a 3D SERS image of our candlestick microstructure (Figure 2C). There is an obvious z-dependent variation of SERS intensities, which gradually decrease from the top nanopillar to the bottom pedestal (Figure 2D, see supporting information for calculation of SERS enhancement factor). This z-dependence is affirmed by the three distinct x-y SERS images extracted at z =1.75 μm, 3.00 μm and 4.25 μm (Figure 2E). The highlighted patterns at z = 4.25 and 3.00 μm resemble the top-view morphology of the candlestick. A small and bright square forms at z = 4.25 μm, with similar width as the nanopillar on the top (Figure 2E-i). A bigger and dimmer square forms at z = 3.00 μm, with similar width as the middle dish (Figure 2E-ii). No obvious SERS image is observed at z = 1.75 μm, which is the height

corresponding to the pedestal region (Figure 2E-iii). Observation from these x-y SERS images tally with the SERS spectra of 4-MBT taken at these planes (Figure 2F). The z-dependence arises primarily from the anisotropic deposition of Ag on the candlestick microstructures during thermal evaporation, in which the topmost nanopillar and the middle dish are coated. The smaller widths of the bottom pedestals are shielded from Ag deposition by the larger middle dish, and are hence SERS-inactive. Moreover, both incident light and Raman scattering fields are coupled with localized surface plasmon resonances, which are supported by the nanopillars as shown in the cathodoluminescence spectrum (Figure 2A). Such an enhancement on surface electromagnetic fields generates stronger SERS signals on the nanopillars as compared with other regions.[36] Our experimental observations collectively show that we can simply tune the pedestal heights to encode information in three-dimensional space. Distinct SERS readouts can be retrieved from the same area at different z focal planes.

Multi-layered 3D Covert Array

Next, we fabricate candlestick microstructures with various heights and demonstrate their potential to encode multi-layer z-dependent SERS information. We begin with a simple 2×2 array consisting of 5-μm and 2.5-μm candlestick microstructures (Figure 3A). These two heights are chosen because a minimum height difference of 2.5 μm is required to prevent signal interferences from successive microstructure heights during SERS imaging (Figure S3). Top-view SEM characterization indicates that these four microstructures are morphologically identical (Figure S4A-ii and Figure 3A-v). However, two layers of information are selectively read out by extracting x-y SERS images at z = 4.25 μm and 1.75 μm, corresponding to SERS signals from the topmost nanopillars of the 5-μm and 2.5-μm microstructures respectively (Figure 3A-iii and iv). Notably,

there is no signal cross-talk at both z-values, especially at z = 1.75 μm where both microstructures are present. As discussed earlier, the presence of the middle dish prevents Ag deposition on the bottom pedestal of the 5-μm microstructure, thus silencing the SERS activity of this microstructure at z = 1.75 μm.

We also compare the SERS-silencing capabilities of the middle dish in the candlestick microstructure against other microstructures with more uniform morphologies (Figure S4). The more uniform microstructures always create signal interferences during SERS imaging at lower z values. As such, by enabling the candlestick microstructure to blend in with the dark background at lower z values, we establish them as ideal architectures to encode multiple layers of information in 3D. Our strategy can also be readily extended to encode molecular information within alternating lines and alphabetical letters using just two sets of candlestick microstructures with two heights (Figure S5). Signal intensities are consistent in the SERS spectra extracted from z = 4.25 μm and 1.75 μm, indicating that the taller candlestick microstructures do not block incoming lasers and outgoing SERS signals from the shorter candlestick microstructures so that molecular information encoded into these two layers can be precisely read out without inter-layer interferences (Figure S5C and D).

We proceed to further demonstrate the high patterning flexibility and decoding accuracy of our 3D SERS encoding strategy by using these 2.5-μm and 5-μm candlestick microstructures to construct complex images. A candlestick array of 247 microstructures covering an area of 72×71 μm^2 encoded with two overlaid images of a butterfly and an orchid flower shows up as random spherical dots in SEM and optical microscopy characterizations (Figure 3B). The butterfly pattern is constructed with 5-μm tall candlesticks and this pattern “lights up” in the SERS x-y image at z = 4.25 μm (Figure 3B-ii). On the other hand, the second set of 2.5-μm tall microstructures reveals the orchid flower pattern in the x-y SERS image at z = 1.75 μm (Figure 3B-iii). There is also no signal

interference observed at both z values among this array of 247 microstructures.

To enhance encoding complexity, an additional third layer of taller 3D microstructures (7.5-μm) can be added into a single array. In a line-array consisting of 7.5-μm, 5-μm and 2.5-μm candlestick-like microstructures, three layers of identification are encrypted into a 6×10 array which cannot be fully revealed under SEM and optical microscopy (Figure 4C-ii and Figure S6B). These three layers are decrypted only by extracting individual x-y SERS images at the corresponding z values of 6.75 μm, 4.25 μm, and 1.75 μm. These z values are unknown to the public and are only accessible by the authorized party (Figure 4A-iii-v). Moreover, the SERS spectra of 4-MBT retrieved from individual nanopillars are spectrally identical with no signal cross talk across the different layers (Figure S7 and Figure 4B). A statistical analysis of 42 SERS spectra taken from three heights show that the SERS intensities of the 1078-cm^{-1} band on nanopillars are uniform and are not affected by their z positions (Figure S5 and S7). As such, the height information cannot be decoded based on different contrast or signal intensities in each SERS images. These attributes collectively demonstrate the Level 3 Security of our security labels in which information can only be fully resolved using advanced 3D SERS imaging technique with knowledge on the label design.

Next, we design and fabricate an 18×23 square array of microstructures spaced 700 nm apart as a complicated 3D anti-counterfeiting security label (Figure 4D). As with previous arrays, we observe no apparent difference among these microstructures from SEM characterization but this array consists of candlesticks with three different heights (7.5-μm, 5-μm and 2.5-μm, Figure 4D-i). In fact, three distinct butterfly patterns are constructed and hidden into this array. X-y SERS imaging at z = 6.75 μm exhibits a small butterfly in the center of the entire array while imaging at z = 4.25 μm reveals a double-layer butterfly (Figure 4D-ii and -iii). A hollow butterfly shows up in the x-y SERS image at z = 1.75 μm (Figure 4D-iv). In anti-counterfeiting terms, these x-y SERS images

serve as three identification layers of a security label made using our 3D encoding strategy. As such, we can arbitrarily encode information in 3D and this ability is in contrast with other 2D SERS security labels which can only encode information within a single 2D plane. Our fabrication protocol allows the fabrication of candlestick microstructures with heights up to 10.5 μm (Figure S8). With a minimal height difference of 2.5 μm between successive layers, we can encode up to four layers of information within the same area to enhance the information density and security level of our security label.

3D SERS Security Codes

Information is highly secured by 3D SERS security labels comprising of our 3D candlestick microstructures because the microstructure heights employed as encryption layer are only accessible to the authorized party. To demonstrate the high security and decoding accuracy of such height encryption, we fabricate two identical arrays comprising 71 candlesticks with heights of 7.5-μm, 5-μm and 2.5-μm (Figure 5). The two arrays appear identical under SEM and optical microscopy (Figure 5A and B). However, the letters “N”, “T”, and “U” are revealed by x-y images in the first array at z = 6.75 μm, 4.25 μm and 1.75 μm respectively, corresponding to the acronym of Nanyang Technological University (Figure 5A-ii-iv). On the other hand, the letters “U”, “T”, and “N” are revealed by x-y images in the second array at the same z values (Figure 5B-ii-iv). The letters “N” and “U” appear in x-y SERS images extracted at different z values because they are constructed by microstructures of different heights in these two arrays.

Apart from high security level of our 3D SERS security labels, a large encoding capacity can be achieved in our 3d SERS encoding platform by using a single type of Raman probe molecule and uniform SERS intensities. Our fabrication method allows a minimal gap of 700 nm between

neighbored candlestick-like structures, so a density of 8466 pillars per inch can be obtained (Figure S9). Moreover, our microscale 3D SERS security labels are encoded with high data density. Fully decoding the hidden information requires SERS imaging techniques with high spatial resolution in three dimensions. Compared with other millimeter- and centimeter-size SERS security labels, our system is more challenging to be counterfeited and thus it is higher in security level.[37]

Flexible 3D Anti-Counterfeiting Security Label

To enhance the applicability of our 3D security labels, we directly fabricate an array of candlestick microstructures on free-standing polyethylene terephthalate (PET) films. PET is popularly used to produce flexible devices due to their high mechanical strengths and flexibility. An array of 2.5-μm and 5-μm candlestick microstructures are fabricated over an area of ~23×38 μm^2 on the PET film. SEM and bright-field microscopic characterization reveal the Arabic number "6" on the PET film (Figure 6A-i and -ii). However, x-y SERS images at z = 1.75 μm and 4.25 μm reveal two overlapping letters "S" and "G" (acronym of Singapore, Figure 6A-iii and -iv). To illustrate the robustness of the 3D security labels, we perform 50 stress cycles on the flexible PET film, where one stress cycle constitutes a bending, flexing, and twisting force (Figure 6B), and compare the SERS readouts of the structures before and after the stress cycles are performed. SEM images reveal the candlestick structures still remain well-defined and upright after the stress cycles are performed, even though the substrate displays multiple strain cracks (Figure 6C). Corresponding SERS images demonstrate that the letter "G" can be read out clearly (Figure 6D), with only an insignificant decrease (~ 20 cps) in SERS intensity (Figure 6E) after 50 stress cycles. The consistency of the SERS images and spectra before and after the stress cycles are performed indicate that this flexible 3D SERS security labels can be easily applied to non-rigid surfaces, such as documents, banknotes,

irregular packages and medicine vials without reducing the decoding accuracy or coding capacity, outperforming and breaking the limitations of current plasmonic security labels that can only be applied to rigid substrates.

Conclusions

In conclusion, we have demonstrated an advanced SERS encoding platform where molecular information is encoded in three dimensions. Moreover, our 3D SERS anti-counterfeiting security labels can be fabricated on both rigid and flexible substrates, widening their potential usage as compared to strategies based on rigid substrates. In terms of anti-counterfeiting application, multiple layers of covert images are hidden into arrays of 3D candlestick microstructures with various heights and they can be selectively revealed by extracting SERS images at specific z values. These z values are unknown to the public and are only accessible to the authorized party. Compared to conventional 2D SERS anti-counterfeiting platforms, our current 3D encoding platform enables up to four-fold denser data encryption along the z-axis using only a single probe molecule within the same 2D area. Our 3D encoding platform exhibits large encoding capacity, high decoding accuracy, and high flexibility by using single type and concentration of probe molecules. Further complexity can be introduced via multiplex encoding platforms to embed multiple probe molecules onto our 3D security labels. In addition, a systematic stability testing can be conducted on these 3D plasmonic security labels to evaluate their long-term stability in air. Platform durability is to be lengthened for practical uses.

Methods

Materials. IP-Dip photoresist with refractive index n≈1.52 (Nanoscribe Inc, Germany) was used as

negative photoresist for two-photon lithography in dip-in laser lithography (DiLL) configuration. 4-methylbenzenethiol (4-MBT, 98%), propylene glycol monomethyl ether acetate, isopropyl alcohol, ethanol were purchased from Sigma-Aldrich. All chemicals were used without further purification. Polyethylene terephthalate (PET) films with the thickness of 100 μm were donated from Innox Higa Singapore PTE. LED.

Fabrication of polymeric anti-counterfeiting structures on glass slides and PET flims. Polymeric nano and/or microstructures were fabricated using direct laser writing system (Nanoscribe Inc., Germany). In the typical experiment, a droplet of IP-Dip monomer was drop-casted on a PET film then polymerized by a computer-assisted femto second pulsed fiber laser with a center wavelength of 780 nm. Polymeric structures were formed according to the pre-defined graphic programs. The Dip-in Laser Lithography (DiLL) process was performed using an inverted microscope with an oil immersion lens (100×, NA 1.3), and a computer-controlled piezoelectric stage. The average laser power around 8 mW and a writing speed at 30 μm/s were used for fabricating polymeric structures on glass slides. An average laser power around 6mW and a writing speed at 40 μm/s were used for fabricating polymeric structures on PET films. Then, unexposed photoresist was removed in propylene glycol monomethyl ether acetate for 10 min, and then samples were immersed into isopropyl alcohol for another 5 min. Samples were blow-dried under N_2.

Metallization of the 3d pillar structures. Ag film was deposited on the substrates using a thermal evaporator. The deposition rate of Ag was 1 Å/s, which was monitored in-situ by a quartz crystal microbalance. Ag tablets with 99.99% purity was purchased from Advent Research Materials, UK.

Ligand exchange reactions. Modification of 4-MBT monolayer was performed by incubating the plasmonic structures in 10 mM 4-MBT ethanol solution for 12 hours. After that, samples were removed and rinsed with copious of ethanol, and dried in nitrogen gas. Owing to a strong Ag-S

coordination bond, 4-MBT was expected to form a self-assembled monolayer (SAM) on the Ag nanostructures.

High speed slit-scanning confocal Raman spectroscopy measurements. SERS spectra and SERS mapping were obtained with the sample mounted on the Ramantouch microspectrometer (Nanophoton Inc, Osaka, Japan). A 532-nm laser was used as an excitation laser. The excitation laser was focused into a line on a sample through a cylindrical lens and an air objective lens (LU Plan Fluor 100× NA 0.9). The back-scattered Raman signal from the line illuminated site was collected with the same objective lens, and a one-dimensional Raman image (1D space and Raman spectra) was obtained with a two-dimensional image sensor (Princeton Instrument, PIXIS 400 BR, -70 °C, 1340 × 400 pixels) at once. At a single acquisition, line-shaped illumination was shone on the sample, where 400 of Raman scattering points were then collected simultaneously in the x-direction. Two-dimensional (2D) x-y and x-z Raman spectral images were obtained by scanning the line-shaped laser focused in single y- and z-direction respectively. The excitation laser power was 0.04 mW on the sample plane. The exposure time for each line and slit width of the spectrometer were 1 s and 50 μm for 2D Raman imaging. The x-y-z SERS image was obtained by combining multiple x-y SERS images taken at various z values with intervals of 500 nm into a single image using an image processing software. To obtain x-y SERS maps at targeted z values, we first focused the laser onto the substrate base (bottom of the 3D microstructures) and define z as “0” at this position. The laser focal plane was then moved from the base of the substrate towards the top of the 3D microstructures by moving the motorized stage. Real time positional changes were tracked on the computer via an attached bright field camera. The distance between the laser focal plane along the 3D microstructures and base of substrate was termed using the numerical z value. x-y mapping at fixed z values was achieved by moving the stage to the targeted z value in the software before

Raman mapping. On the other hand, x-z mapping was achieved by a programmed movement of the stage so that the laser was scanned from the base to the top of the 3D microstructures.

Cathodoluminescence hyperspectral imaging. Quantitative cathodoluminescence was carried out using an Attolight Rosa 4634 microscope, which tightly integrates a high-speed achromatic reflective lens (N.A. 0.72) within the objective lens of a field emission gun scanning electron microscope (FEG-SEM). Cathodoluminescence was spectrally resolved with a Czerny-Turner spectrometer (Horriba-JY iHR320, 320 mm focal length, 150 grooves/mm grating) and measured with an Andor Newton EM-CCD (EM-970P-BV). Electron beam energies of 9 kV were used to excite the samples. The beam dwell time was set to 0.2 s.

Characterization. Scanning electron microscopy (SEM) was performed using a JEOL-JSM-7600F with an accelerate voltage of 5 kV.

Acknowledgements

X.Y.L. thanks the financial support from National Research Foundation, Singapore (NRF-NRFF2012-04), Singapore Ministry of Education, Tier 1 (RG21/16) and Tier 2 (MOE2016-T2-1-043) grants, and Nanyang Technological University. M.R.L thanks the support from Nanyang Presidential Graduate Scholarship.

Supporting Information. AFM images; zoom-in SEM images; minimal difference in height of candlestick-like microstructures in two layers; comparison on SERS readouts of 3D security labels constructed by different 3D microstructures; two-layer 3D SERS security labels; SEM and optical microscopic images of two-layer overlaid patterns of an orchid and a butterfly and three-layer alternating line-pattern; SERS spectra of 4-MBT taken from three-layer alternating line-pattern; 3D

candlestick-like microstructures of different heights; limit of microstructure density; calculation of enhancement factor (EF) of 3D SERS substrate.

REFERENCES

1. Kumar, K.; Duan, H.; Hegde, R. S.; Koh, S. C.; Wei, J. N.; Yang, J. K., Printing Colour at the Optical Diffraction Limit. *Nat. Nanotechnol.* **2012**, *7*, 557-61.
2. Goh, X. M.; Zheng, Y.; Tan, S. J.; Zhang, L.; Kumar, K.; Qiu, C. W.; Yang, J. K., Three-Dimensional Plasmonic Stereoscopic Prints in Full Colour. *Nat. Commun.* **2014**, *5*, 5361.
3. Tan, S. J.; Zhang, L.; Zhu, D.; Goh, X. M.; Wang, Y. M.; Kumar, K.; Qiu, C. W.; Yang, J. K., Plasmonic Color Palettes for Photorealistic Printing with Aluminum Nanostructures. *Nano Lett.* **2014**, *14*, 4023-9.
4. Miyata, M.; Hatada, H.; Takahara, J., Full-Color Subwavelength Printing with Gap-Plasmonic Optical Antennas. *Nano Lett.* **2016**, *16*, 3166-72.
5. Huang, Y. W.; Chen, W. T.; Tsai, W. Y.; Wu, P. C.; Wang, C. M.; Sun, G.; Tsai, D. P., Aluminum Plasmonic Multicolor Meta-Hologram. *Nano Lett.* **2015**, *15*, 3122-7.
6. Gu, Y.; Zhang, L.; Yang, J. K.; Yeo, S. P.; Qiu, C. W., Color Generation Via Subwavelength Plasmonic Nanostructures. *Nanoscale* **2015**, *7*, 6409-19.
7. Li, X.; Chen, L.; Li, Y.; Zhang, X.; Pu, M.; Zhao, Z.; Ma, X.; Wang, Y.; Hong, M.; Luo, X., Multicolor 3d Meta-Holography by Broadband Plasmonic Modulation. *Sci. Adv.* **2016**, *2*, e1601102.
8. Olson, J.; Manjavacas, A.; Liu, L.; Chang, W.-S.; Foerster, B.; King, N. S.; Knight, M. W.; Nordlander, P.; Halas, N. J.; Link, S., Vivid, Full-Color Aluminum Plasmonic Pixels. *Proc. Natl. Acad. Sci.* **2014**, *111*, 14348-14353.
9. Cui, Y.; Phang, I. Y.; Lee, Y. H.; Lee, M. R.; Zhang, Q.; Ling, X. Y., Multiplex Plasmonic Anti-Counterfeiting Security Labels Based on Surface-Enhanced Raman Scattering. *Chem. Commun.* **2015**, *51*, 5363-6.
10. Cui, Y.; Phang, I. Y.; Hegde, R. S.; Lee, Y. H.; Ling, X. Y., Plasmonic Silver Nanowire Structures for Two-Dimensional Multiple-Digit Molecular Data Storage Application. *ACS Photonics* **2014**, *1*, 631-637.
11. Cui, Y.; Hegde, R. S.; Phang, I. Y.; Lee, H. K.; Ling, X. Y., Encoding Molecular Information in Plasmonic Nanostructures for Anti-Counterfeiting Applications. *Nanoscale* **2014**, *6*, 282-8.
12. Liu, Y.; Lee, Y. H.; Zhang, Q.; Cui, Y.; Ling, X. Y., Plasmonic Nanopillar Arrays Encoded with Multiplex Molecular Information for Anti-Counterfeiting Applications. *J. Mater. Chem. C* **2016**, *4*, 4312-4319.
13. Zhang, Q.; Lee, Y. H.; Phang, I. Y.; Lee, C. K.; Ling, X. Y., Hierarchical 3d Sers Substrates Fabricated by Integrating Photolithographic Microstructures and Self‐Assembly of Silver Nanoparticles. *Small* **2014**, *10*, 2703-2711.
14. Liu, X.; Wang, J.; Tang, L.; Xie, L.; Ying, Y., Flexible Plasmonic Metasurfaces with User-Designed Patterns for Molecular Sensing and Cryptography. *Adv. Funct. Mater.* **2016**, *26*, 5515-5523.
15. Li, D.; Tang, L.; Wang, J.; Liu, X.; Ying, Y., Multidimensional Sers Barcodes on Flexible Patterned Plasmonic Metafilm for Anticounterfeiting Applications. *Adv. Opt. Mater.* **2016**, *4*, 1475-1480.
16. Zijlstra, P.; Chon, J. W.; Gu, M., Five-Dimensional Optical Recording Mediated by Surface Plasmons in Gold Nanorods. *Nature* **2009**, *459*, 410-3.
17. Li, X.; Lan, T. H.; Tien, C. H.; Gu, M., Three-Dimensional Orientation-Unlimited Polarization

Encryption by a Single Optically Configured Vectorial Beam. *Nat. Commun.* **2012**, *3*, 998.
18. Wu, D. M.; Garcia-Etxarri, A.; Salleo, A.; Dionne, J. A., Plasmon-Enhanced Upconversion. *J. Phys.Chem. Lett.* **2014**, *5*, 4020-31.
19. Kim, J.; Yun, J. M.; Jung, J.; Song, H.; Kim, J. B.; Ihee, H., Anti-Counterfeit Nanoscale Fingerprints Based on Randomly Distributed Nanowires. *Nanotechnology* **2014**, *25*, 155303.
20. Haglmüller, J.; Alguel, Y.; Mayer, C.; Matyushin, V.; Bauer, G.; Pittner, F.; Leitner, A.; Aussenegg, F.; Schalkhammer, T. **2004**, January. Cluster optical coding–from biochips to counterfeit security. In Proc. of SPIE Vol (Vol. 5339, p. 653).
21. Ditlbacher, H.; Krenn, J.; Lamprecht, B.; Leitner, A.; Aussenegg, F., Spectrally Coded Optical Data Storage by Metal Nanoparticles. *Opt. Lett.* **2000**, *25*, 563-565.
22. Park, K.; Jung, K.; Kwon, S. J.; Jang, H. S.; Byun, D.; Han, I. K.; Ko, H., Plasmonic Nanowire-Enhanced Upconversion Luminescence for Anticounterfeit Devices. *Adv. Funct. Mater.* **2016**, *26*, 7836-7846.
23. Ravi, S.; Raghunathan, A.; Kocher, P.; Hattangady, S., Security in Embedded Systems: Design Challenges. *ACM Transactions on Embedded Computing Systems (TECS)* **2004**, *3*, 461-491.
24. Zhang, C.-y.; Lu, Y.; Zhao, B.; Hao, Y.-w.; Liu, Y.-q., Facile Fabrication of Ag Dendrite-Integrated Anodic Aluminum Oxide Membrane as Effective Three-Dimensional Sers Substrate. *Appl. Surf. Sci.* **2016**, *377*, 167-173.
25. Zhang, C., et al., Gold@Silver Bimetal Nanoparticles/Pyramidal Silicon 3d Substrate with High Reproducibility for High-Performance SERS. *Sci. Rep.* **2016**, *6*, 25243.
26. Vantasin, S.; Ji, W.; Tanaka, Y.; Kitahama, Y.; Wang, M.; Wongravee, K.; Gatemala, H.; Ekgasit, S.; Ozaki, Y., 3d Sers Imaging Using Chemically Synthesized Highly Symmetric Nanoporous Silver Microparticles. *Angew. Chem. Int. Ed. Engl.* **2016**, *55*, 8391-5.
27. Urban, M. J.; Dutta, P. K.; Wang, P.; Duan, X.; Shen, X.; Ding, B.; Ke, Y.; Liu, N., Plasmonic Toroidal Metamolecules Assembled by DNA Origami. *J. Am. Chem. Soc.* **2016**, *138*, 5495-8.
28. Tabatabaei, M.; Najiminaini, M.; Davieau, K.; Kaminska, B.; Singh, M. R.; Carson, J. J. L.; Lagugné-Labarthet, F., Tunable 3d Plasmonic Cavity Nanosensors for Surface-Enhanced Raman Spectroscopy with Sub-Femtomolar Limit of Detection. *ACS Photonics* **2015**, *2*, 752-759.
29. Yang, S.; Lapsley, M. I.; Cao, B.; Zhao, C.; Zhao, Y.; Hao, Q.; Kiraly, B.; Scott, J.; Li, W.; Wang, L., Large‐Scale Fabrication of Three‐Dimensional Surface Patterns Using Template‐Defined Electrochemical Deposition. *Adv. Funct. Mater.* **2013**, *23*, 720-730.
30. Kondo, T.; Miyazaki, H.; Nishio, K.; Masuda, H., Surface-Enhanced Raman Scattering on Multilayered Nanodot Arrays Obtained Using Anodic Porous Alumina Mask. *J. Photochem. Photobiol. A* **2011**, *221*, 199-203.
31. Cinel, N. A.; Bütün, S.; Ertaş, G.; Özbay, E., 'Fairy Chimney'‐Shaped Tandem Metamaterials as Double Resonance Sers Substrates. *Small* **2013**, *9*, 531-537.
32. Zhao, L.; Kelly, K. L.; Schatz, G. C., The Extinction Spectra of Silver Nanoparticle Arrays: Influence of Array Structure on Plasmon Resonance Wavelength and Width. *J. Phys. Chem. B* **2003**, *107*, 7343-7350.
33. Ghosh, S. K.; Pal, T., Interparticle Coupling Effect on the Surface Plasmon Resonance of Gold Nanoparticles: From Theory to Applications. *Chem. Rev.* **2007**, *107*, 4797-4862.
34. Haynes, C. L.; McFarland, A. D.; Zhao, L.; Van Duyne, R. P.; Schatz, G. C.; Gunnarsson, L.; Prikulis, J.; Kasemo, B.; Käll, M., Nanoparticle Optics: The Importance of Radiative Dipole Coupling in Two-Dimensional Nanoparticle Arrays. *J. Phys. Chem. B* **2003**, *107*, 7337-7342.
35. Koh, A. L.; Bao, K.; Khan, I.; Smith, W. E.; Kothleitner, G.; Nordlander, P.; Maier, S. A.; McComb, D. W., Electron Energy-Loss Spectroscopy (Eels) of Surface Plasmons in Single Silver Nanoparticles and Dimers: Influence of Beam Damage and Mapping of Dark Modes. *ACS Nano* **2009**, *3*, 3015-3022.

36. Schlücker, S., Surface-Enhanced Raman Spectroscopy: Concepts and Chemical Applications. *Angew. Chem. Int. Ed.* **2014**, *53*, 4756-4795.
37. Liu, X.; Wang, J.; Tang, L.; Xie, L.; Ying, Y., Flexible Plasmonic Metasurfaces with User-Designed Patterns for Molecular Sensing and Cryptography. *Adv. Funct. Mater.* **2016**, *26*, 5515-5523.

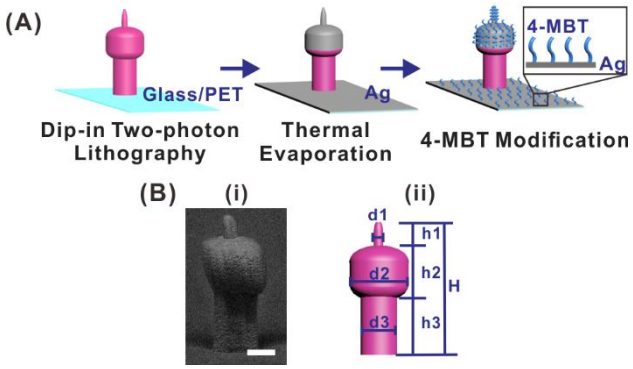

Figure 1. Fabrication and characterization of 3D candlestick-like microstructures. (A) Polymeric 3D candlestick-like microstructure is fabricated using direct laser writing, and is subsequently deposited with Ag via thermal evaporation. Finally, a monolayer of 4-methylbenzenethiol (4-MBT) is functionalized onto the Ag candlestick-like microstructures as molecular probe. (B) (i) side-view SEM image and (ii) scheme demonstrating a 5-μm candlestick-like microstructure in which nanopillar height (h1) = 1 μm, dish height (h2) = 2 μm, pedestal height (h3) = 2 μm, total height (H) = 5 μm, nanopillar diameter (d1) = 500 nm, dish diameter (d2) = 2.3 μm, pedestal diameter (d3) = 1.7 μm. The scale bar represents 1 μm.

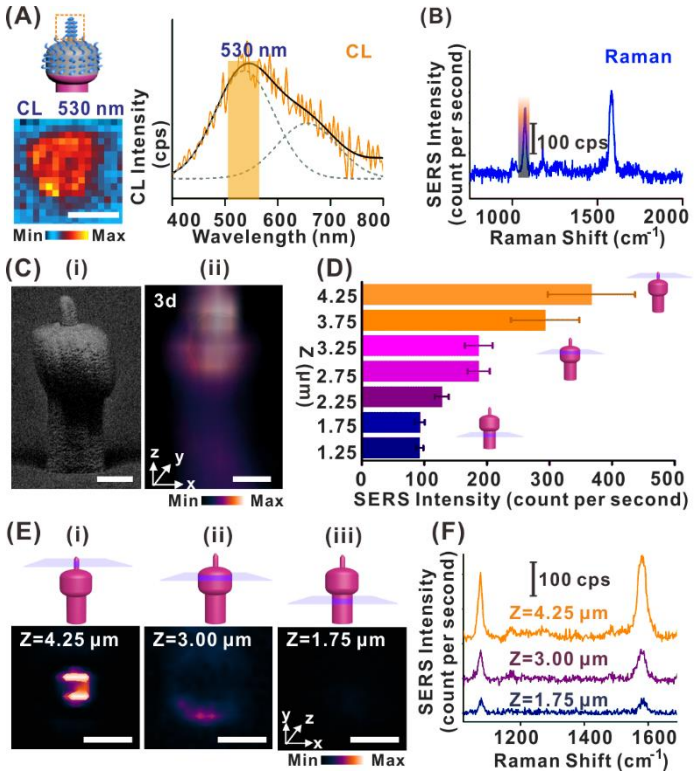

Figure 2. Z-dependent SERS readouts on a single 3D candlestick-like microstructure. (A) A cathodoluminescence (CL) map and spectrum taken from a nanopillar of candlestick-like microstructure. CL map is acquired at wavelength window centered at ~530 nm. (B) A typical SERS spectrum taken from nanopillar on candlestick-like microstructure. (C) (i) side-view SEM and (ii) 3D SERS images. SERS images are derived using the 1078 cm^{-1} vibrational band of 4-MBT. (D) SERS intensity plot of 4-MBT obtained at different z-locations ranging from Z=4.25 to Z =1.25 μm. (E, F) X-y SERS images and SERS spectra obtained at various z-focal planes, where (i) Z=4.25 μm, (ii) Z=3.00 μm and Z=1.75 μm, respectively. Scale bar in (A) represents 500 nm and other scale bars represent 1 μm.

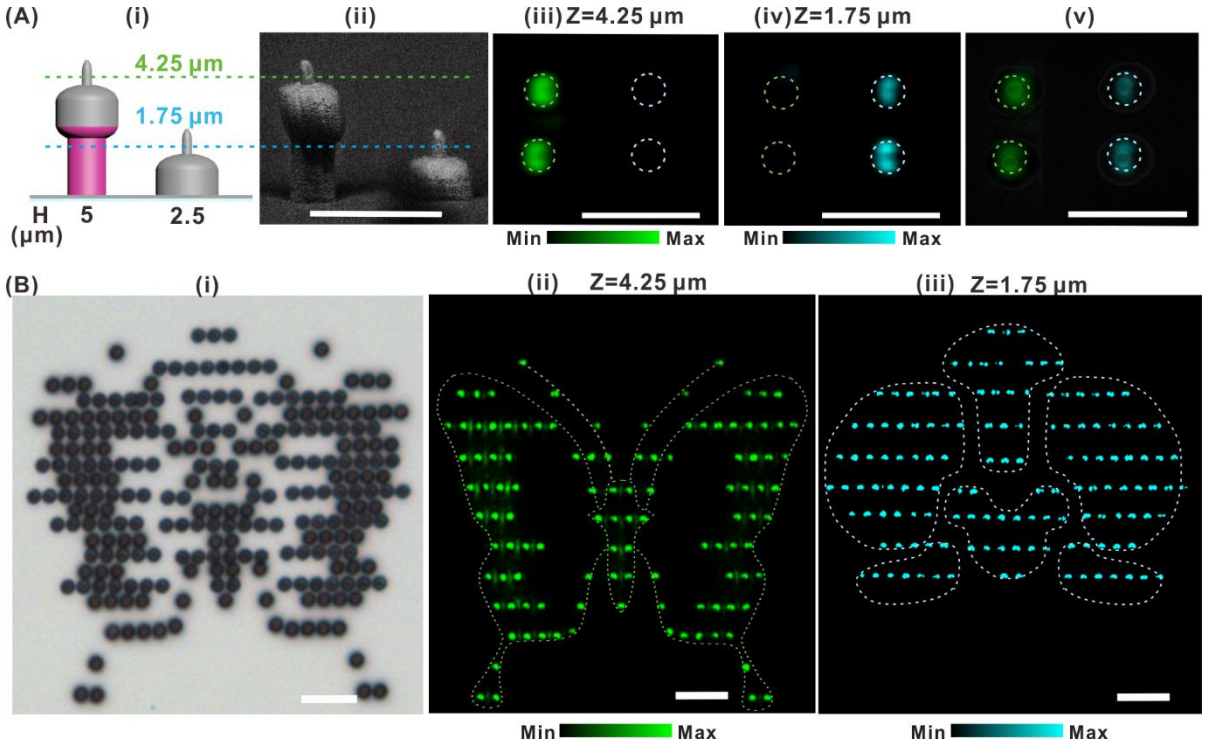

Figure 3. Two-layered 3D SERS security labels. (A) (i) Scheme, (ii) side-view SEM image of a 2×2 array. 2D x-y SERS images acquired at focal planes of (iii) Z=4.25 μm and (iv) Z=1.75 μm. (v) Overlaid SERS images with a top-view SEM image of the 2×2 candlestick-like microstructure array. Scale bars represent 5 μm. (B)(i) An optical microscope image of overlapped patterns of an orchid and a butterfly, and their respective x-y SERS images acquired at focal planes of (ii) Z=4.25 μm and (ii) Z=1.75 μm. Note that the orchid and butterfly patterns are constructed using 2.5-μm and 5-μm candlestick-like structures, respectively. Scale bars represent 10 μm.

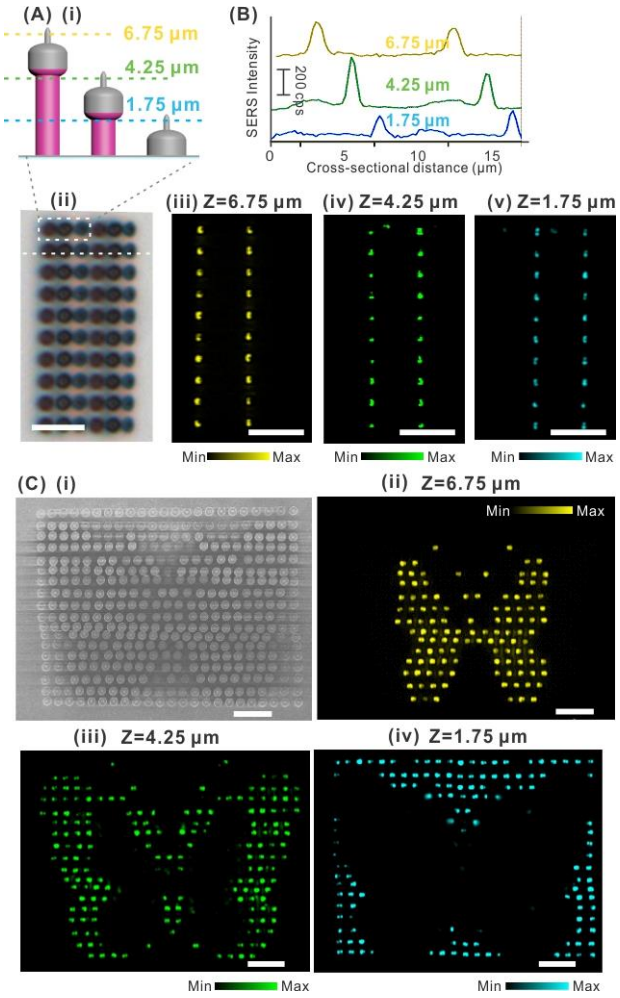

Figure 4. Three-layered 3D SERS security labels. (A) Alternating line-pattern which are constructed by 2.5-μm, 5-μm and 7.5-μm structures. (i) Scheme, (ii) optical microscopic image and 2D x-y SERS images acquired at focal planes of (iii) Z=6.75 μm, (iv) 4.25 μm and (v) 1.75 μm. (B) cross-sectional SERS intensity profile along y-direction as labeled in A-ii. (C) Overlapped patterns of three butterflies which are constructed of 2.5-μm, 5-μm and 7.5-μm structures. (i) SEM and 2D x-y SERS images acquired at focusing planes where (ii) Z=6.75 μm, (iii) 4.25 μm and (iv) 1.75 μm. SERS images and intensity profiles are derived using the 1078 cm^{-1} vibrational band of 4-MBT. All scale bars represent 10 μm.

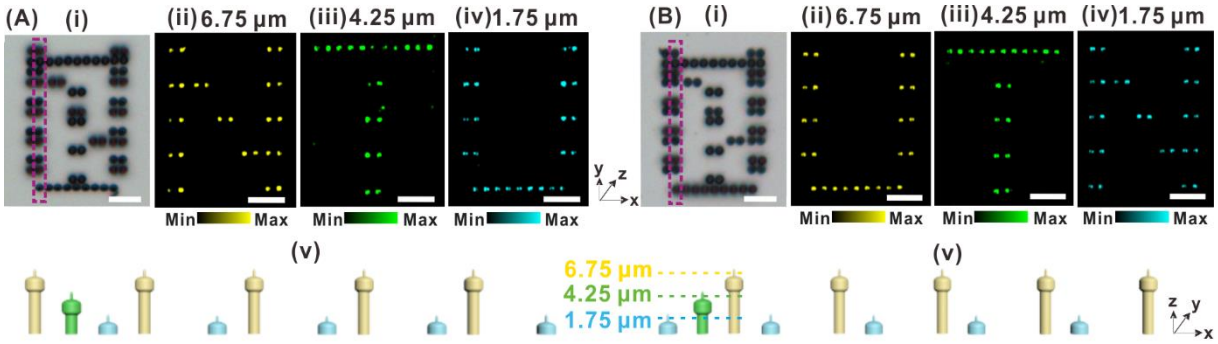

Figure 5. 3D SERS security codes. (A) "NTU" security label and (B) "UTN" security label with their respective (i) Optical microscopic images, (ii-iv) x-y SERS images obtained at Z=6.75, 4.25 and 1.75 μm, (v) schemes showing the arrangement of microstructures at the second vertical line in two security labels. SERS images are derived using the 1078 cm^{-1} vibrational band of 4-MBT. All scale bars represent 10 μm.

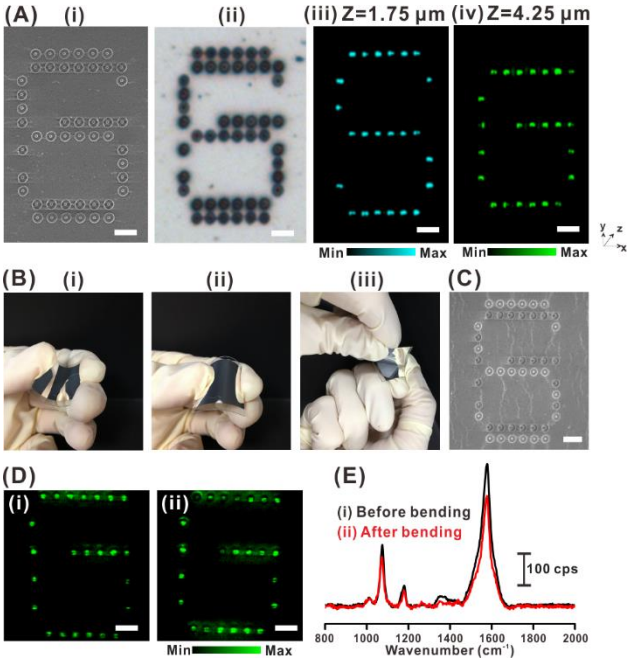

Figure 6. Flexible 3D SERS security labels. (A) (i) SEM, (ii) optical microscopic images and x-y SERS readouts of a security label of overlaid letters "SG" when imaging at (iii) Z=1.75 µm and (iv) Z=4.25 µm. (B) Camera photos of a flexible 3D SERS security label (i) at bending (ii) flexing and (iii) twisting forces. Performing each action in (B) (i), (ii) and (iii) once, constitutes one mechanical stress cycle. (C) SEM image of the flexible substrate after 50 mechanical stress cycles. (D) SERS images and the (E) corresponding SERS spectra of the letter "G" (i) before and (ii) after 50 mechanical stress cycles. SERS images and spectra are both derived using the 1078 cm^{-1} vibrational band of 4-MBT. All scale bars represent 5 µm.

For Table of Contents Use Only

Flexible Three-Dimensional Anti-Counterfeiting Plasmonic Security Labels: Utilizing Z-Axis-Dependent SERS Readouts to Encode Multi-Layered Molecular Information

Yejing Liu,[1] Yih Hong Lee,[1] Mian Rong Lee,[1] Yijie Yang,[1] Xing Yi Ling[1]*

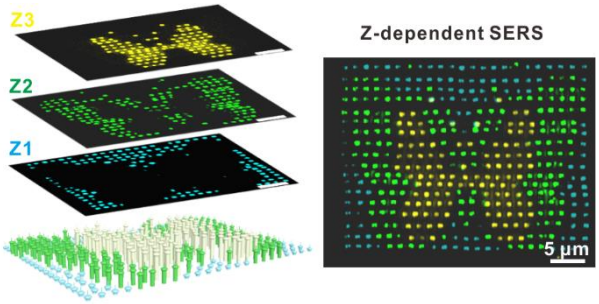

We demonstrate a 3D SERS anti-counterfeiting platform to extend "layered security" capabilities from 2D to 3D, by combining 3D candlestick microstructures with 3D SERS imaging to fully resolve multiple layers of encoded information within the same 2D area along the z-axis.